Neurotherapeutics (2017) 14:358–371
DOI 10.1007/s13311-017-0520-4

REVIEW

Convection-Enhanced Delivery

A. M. Mehta[1] · **A. M. Sonabend**[1] · **J. N. Bruce**[1]

Published online: 15 March 2017
© The American Society for Experimental NeuroTherapeutics, Inc. 2017

Abstract Convection-enhanced delivery (CED) is a promising technique that generates a pressure gradient at the tip of an infusion catheter to deliver therapeutics directly through the interstitial spaces of the central nervous system. It addresses and offers solutions to many limitations of conventional techniques, allowing for delivery past the blood–brain barrier in a targeted and safe manner that can achieve therapeutic drug concentrations. CED is a broadly applicable technique that can be used to deliver a variety of therapeutic compounds for a diversity of diseases, including malignant gliomas, Parkinson's disease, and Alzheimer's disease. While a number of technological advances have been made since its development in the early 1990s, clinical trials with CED have been largely unsuccessful, and have illuminated a number of parameters that still need to be addressed for successful clinical application. This review addresses the physical principles behind CED, limitations in the technique, as well as means to overcome these limitations, clinical trials that have been performed, and future developments.

Key Words Convection-enhanced delivery · Malignant gliomas · Drug delivery · Technique · Central nervous system · Blood–brain barrier

✉ J. N. Bruce
jnb2@cumc.columbia.edu

[1] Department of Neurological Surgery, Columbia University Medical Center, New York, NY 10032, USA

Introduction

In spite of significant advances in surgery, imaging, and adjuvant therapy, the average prognosis for glioblastoma multiforme (GBM) is only about 13 months, with a 2-year survival rate of 27%, and a 5-year survival rate of 5.1% [1–4]. This poor prognosis can be attributed to a number of challenges historically related to treating neurological diseases. Chief amongst these challenges is the blood–brain barrier (BBB), which is largely responsible for the gap between scientific advances and improvement of outcomes for many neurological diseases [5–9]. In addition, many forms of delivery, including systemic delivery (intravenously or oral), are limited by the blood–cerebrospinal fluid (CSF) barrier and by systemic toxicities [10, 11]. These limitations make it difficult to achieve therapeutic concentrations of agents in targeted areas of the brain.

However, over the course of the past few decades, convection-enhanced delivery (CED) has emerged as a promising delivery technique that addresses many of the aforementioned issues.

This review provides an introduction to CED, describing its appeal, the biological and physical principles surrounding CED, its physical limitations, a synopsis of noteworthy CED clinical trials, and future improvements in the technique.

Overview

Edward Oldfield's group at the National Institute of Health developed CED in the early 1990s [12–15]. The technique was proposed as a method to deliver drugs that were either limited by the BBB or were too large to diffuse effectively [16]. The appeal of CED is multifold; it allows for bypassing of the BBB, targeted delivery, and perfusion of deep brain

targets both near and downstream of the site of infusion [6, 12–14, 17–24]. CED is especially relevant in the treatment of malignant gliomas, as recurrence generally occurs within centimeters of the original tumor [25], and CED can reach the peritumoral region and beyond [16]. CED allows for a predictable, homogenous, "square-shaped" distribution, and unlike diffusive therapies, which are limited by concentration gradients, it allows for direct access to the tumor bed, resulting in high local concentrations of drug with minimal systemic absorption [10, 12, 26–29]. In addition, CED is applicable to a wide range of compounds, as evidenced by a number of studies using chemotherapeutic agents, low-molecular-weight imaging tracers, proteins, viruses and virus-shaped particles, liposomes, and nanoparticles [24, 30–32]. In addition, it is applicable in solid-tissue tumors in peripheral organs such as the prostate and the liver [33].

The BBB

The BBB isolates systemic circulation from the brain parenchyma. It exists along cerebral capillaries and contains tight junctions that do not exist in systemic circulation. The BBB restricts the passage of many substances, including bacteria, large molecules (molecular weight > 40 kD), and hydrophilic molecules, primarily to protect the brain from infections and toxic substances. Substances like nutrients and waste metabolites are actively transported across the BBB. Many of the promising therapeutics for central nervous system (CNS) diseases are large molecules, their size preventing their diffusion through the BBB and the brain interstitium [34]. Those therapies that are able to penetrate the CNS often cannot reach sufficiently high concentrations, as the required systemic concentrations are unacceptably toxic [11].

Physical Principles

CED is unlike other delivery techniques in the biophysical properties that underlie its movement within the CNS as reviewed by Lonser et al. [18] These principles are summarized as follows.

CED utilizes bulk flow rather than diffusion. Diffusive flow relies on a concentration gradient and operates according to Fick's law, $J = -D \nabla C$, where D is tissue diffusivity and ∇C is the concentration gradient. Essentially, this principle states that molar flux is proportional to the concentration gradient multiplied by a coefficient (tissue diffusivity). This coefficient is dependent on molecular weight. Therefore, large therapeutic agents take a long time to diffuse and also require unhealthily high concentrations to drive their flow. Additionally, these agents only achieve a tissue penetration of a few millimeters. In contrast, bulk flow distributes via a pressure gradient, and is described by Darcy's law: $v = -K \nabla p$. This law asserts that the velocity of the molecule is directly proportional to the pressure gradient (∇p) and the hydraulic conductivity (K). Therefore, CED does not require unwieldy concentrations to achieve therapeutic levels in the brain parenchyma [19].

Process and Characteristics of CED

For clinical use of CED, one or more catheters are stereotactically inserted through a burr hole into the interstitial spaces of the brain using image guidance (Fig. 1). To create the pressure gradient and drive the flow, an infusion pump is connected to the catheter(s), and the agent is infused directly into the extracellular space of the brain, while displacing the extracellular fluid [11]. The interstitial pathways in the brain allow for convective transport independent of molecule size. However, CED is limited by physical barriers like pial surfaces. The infusion rates typically range from 0.1 to 10 μl/min and the distribution from a single point source results in an elliptical-to-spherical distribution [11]. With CED, the agent can achieve tissue penetration of up to a few centimeters, unlike diffusive therapies, which can only achieve a depth of a few millimeters [16, 18, 36]. The direct infusion of agent into the interstitial space is what allows CED to bypass the BBB. The most effective agents for CED are those that are not well transported across the BBB, as they will not travel from the interstitium back across the BBB into systemic circulation, thus minimizing systemic toxicity [18]. In addition, CED is less likely to cause toxicity to surrounding brain tissue, as the concentration fall off at the border is steep [11].

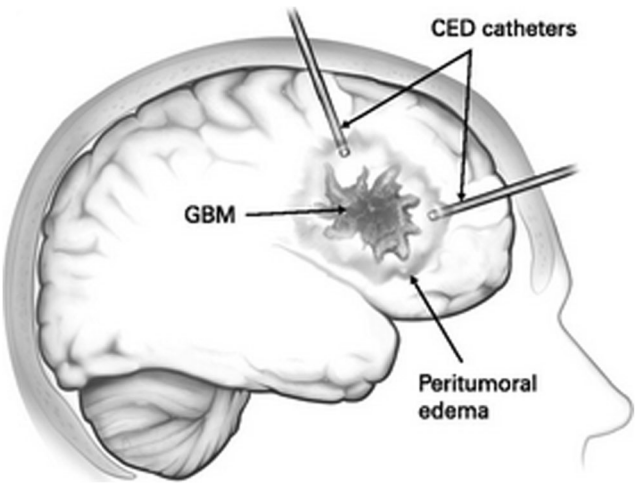

Fig. 1 The surgeon inserts 1 or more catheters through bur holes into the interstitial spaces of the brain. A pressure gradient is generated using an infusion pump, and the agent displaces extracellular fluid after being directly infused into the extracellular space. The tumor is often highly vascularized, and this, as well as a number of factors, can affect the delivery of the infusate (white matter *vs* gray matter, backflow, etc.) Figure printed with permission from the *Journal of Clinical Oncology* [35] CED = convection-enhanced delivery; GBM = glioblastoma multiforme

Physical Limitations

However, CED is not without limitations, and as the technique has developed, a number of physical limitations have been noted and addressed. Among these are many of the traditional variables related to pharmacology including drug half-life and tissue clearance rates, as well as those specific to CED [37]. These include backflow, air bubbles, limitations surrounding flow within brain tissue, white matter edema, target heterogeneity, active tumors/BBB disruption, challenges in the ratio of volume of infusion to the volume of distribution, and, finally, flow rate.

Backflow

Backflow, also known as reflux, occurs along the catheter's insertion tract if the catheter has mechanically disrupted the tissue enough to allow a void to form along the outer wall. A fluid-filled gap between the needle and surrounding tissue forms, through which the infusate can easily flow rather than entering the surrounding tissue (Fig. 2) [39]. Intrinsic backflow occurs when pressure associated with the infusion pushes against the tissues, separating them from the catheter. The shear forces in the tissue balance the pressure field and retrograde axial flow stops. Both types of backflow can be issues in that they allow infusate to exit the target, causing spreading of the agent into unintended areas of the brain [39, 40]. This can lead to a decrease in the dose, and can be especially detrimental during cortical infusions, as it may lead to spread into the subarachnoid space with subsequent widespread distribution through the CSF [16]. The causes of backflow are myriad, but it has been associated with the presence of air bubbles, pressure spikes during the infusion, the catheter insertion technique, and the catheter design. Soft catheters are less likely to cause mechanical disruption and thus backflow [40]. Also, the use of a thin catheter has been shown to be beneficial in overcoming backflow [14], and new "step-design" catheters have been developed to overcome the issues associated with a thin catheter (i.e., floppiness) [41]. In addition, porous-membrane catheters and valve-tip catheter designs have been thought to alleviate occlusions at the end port, thus decreasing pressure spikes and resultant backflow [40].

Air Bubbles

Air bubbles are not inherently a health hazard, but they can disrupt the flow of the infused agent causing unpredictable flow patterns, and can also contribute to backflow [40]. Additionally, air presents an obstacle when attempting to use image guidance for real time monitoring, which is an important step in the effective deployment of CED. Air in the infusion line can alter the local measurement of the infusion pressure as well as the volume of the dye being used. In addition, it may cause local tissue disruption, thus affecting distribution of the infusate [40]. Priming the cannula before insertion into the brain prevents air bubbles from occurring at the end of the catheter tip [42].

Pathologic Conditions

Pathologic scenarios (i.e., active tumors) and postoperative tissue alterations present further challenges in the effective use of CED [16, 37, 43–48]. Malignant gliomas present issues given their increased interstitial pressure related to peritumoral edema, and heterogeneous distribution of blood vessels. The excessive vascularity of active tumors can results in the loss of infusate to circulation. Also, the infusate can follow the trajectory of the vasculature, disrupting its intended distribution pattern [33, 49]. The increased interstitial pressure of the tumors can diminish the pressure gradient that drives convective

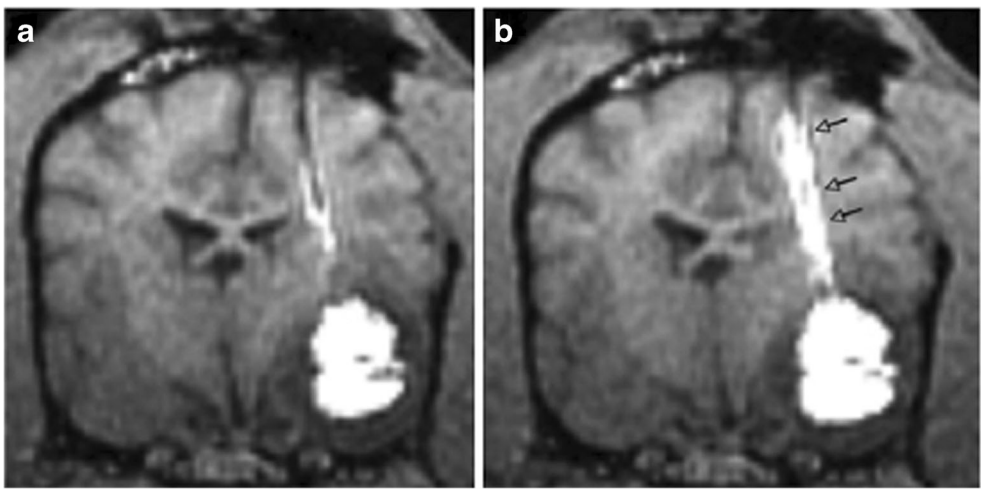

Fig. 2 Reflux at high infusion rates. This 1.5-T magnetic resonance T1-weighted spoiled gradient image shows (A) little reflux at an infusion rate of 5 μl/min but (B) significant reflux (marked by the arrowheads) along the cannula at 8 μl/min. The infusion was done using a reflux-resistant catheter, on a spontaneous canine piriform lobe tumor, and the infusate being delivered was Gadoteridol-labeled neutral nanoliposomes. Figure printed with permission from *Neurotherapeutics* [38]

flow, making it difficult for infusate to access the interstitium during CED [33]. Infusion into, or around, tumors with excessive necrotic tissue can cause pooling of drug, resulting in unequal drug distribution and loss of drug to nonviable tissue [50]. Similar considerations should be made when infusion involves tumors with cystic regions, as well as those in close proximity to ventricles as these may similarly cause loss of drug, either to nonviable tissue or to CSF [51]. Additionally, tumor tissues may be fibrous or have thick scarring from previous therapeutic interventions, which could affect successful flow patterns. In addition, changes that take place in the peritumoral region have been proposed to impede the distribution of large molecules, reducing their volume of distribution (Vd). Distance between catheter tip and resection cavity or other CSF spaces can influence convection. Recently conducted studies have employed guidelines to place catheters at least 2 cm from any brain surface and 1 cm from any cavity [37, 52].

Flow Direction, Rates, Vd, and Vi

The Vd to volume of infusion ratio (Vd:Vi) is a key parameter in the successful deployment and development of CED, as knowing this value for any given anatomical location and type of tumor allows prediction of the required Vi [53]. In general, the Vd is approximately linear to infusion, even for large molecules (80 kD; Fig. 3) [11, 12]. However, this relationship is altered in a number of situations. Excessive flow rates can alter the Vd:Vi ratio. Studies have shown that at rates of greater than 0.5 to 1 μl/min, significant backflow occurs, thus rendering the Vd independent from the Vi [6]. The stability and size of the molecule of interest also play a role in the Vd:Vi ratio. This involves the molecule's lipophilicity, its susceptibility to enzymatic degradation, and the extent to which it binds to cell surface receptors. Excessive binding to receptors can be overcome by saturating the receptors with excess ligands, and there has been some success when the agent is co-infused with heparin [11, 53, 54]. It was previously believed that molecules larger than immunoglobulin G could not pass through the extracellular matrix. However, more recent studies have shown that infusion of adenoid-associated virus and liposomes can be associated with large volumes of distribution [55, 56]. Recent and future developments will help optimize Vd, including reducing backflow and accounting for tissue clearance and metabolism [12, 14, 37, 57, 58].

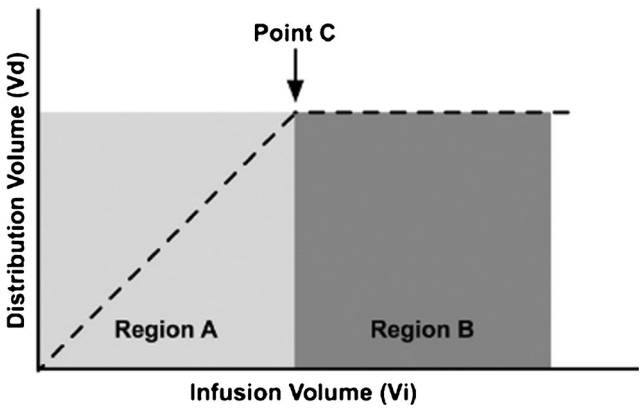

Fig. 3 Relationship between volume of infusion (Vi) and volume of distribution (Vd), both in the absence and presence of reflux. A normal pattern is shown in Region A, in which the Vd increases linearly with Vd. Point C shows the point at which reflux begins, and in Region B, despite an increase in Vi, Vd does not change. Figure printed with permission from *Neurotherapeutics* [38]

Direction of flow is determined not only by the direction of the pressure gradient, but also by resistance to flow. The resistance to flow is both direction-dependent (anisotropic), as well as location-dependent (heterogeneous), and the properties of white *versus* gray matter can dictate flow and thus Vd:Vi [16]. White matter shows less resistance to bulk flow, while gray matter exhibits more regional homogeneity [37, 59–61]. Flow within white matter tracts also differs based on the direction of the tracts [37, 62, 63]. The increased permeability is exaggerated in situations of preexisting edema (i.e., malignancy). Mathematical models and tracer studies in clinical trials have illustrated the preferential movement of infusate along the path of pre-existent white matter edema, which leads to an unpredictability in the Vd:Vi ratio [37, 61]. In the absence of pre-existing edema, edema forms around the catheter, essentially inducing tissue homogeneity. This presents a similar issue in that the flow can be dictated by the edema [16]. In summary, properties unique to white matter can lead to undesirable, and unpredictable flow patterns.

Clinical Trials

A number of clinical trials have been performed, with variable levels of success (Table 1).

Tumor Clinical Trials

TF-CRM107

The first clinical trial using CED was conducted by Edward Oldfield's group at the National Institutes of Health [64]. The chemotherapeutic agent used in this study was an agent selective for the transferrin receptor, TF-CRM107. This agent is a conjugate protein of diphtheria toxin with a point mutation linked via a theioester bond to human transferrin [66, 67]. This was used because many *in vitro* and *in vivo* studies have demonstrated the upregulation of transferrin receptor in rapidly dividing cells, owing to its elevated demand for iron

Table 1 Summary of clinical trials that have been performed recently or are currently ongoing

Trial	Investigators (year)	Agent	Phase	Target disease	Current status	ClinicalTrials.gov identifier
Tumor regression with regional distribution of the targeted toxin TF-CRM107 in patients with malignant brain tumors	Laske et al., 1997 [64]	TF-CRM107	0/I	Refractory recurrent malignant tumor	Completed	NA
Interstitial infusion of IL13-PE38QQR cytotoxin in recurrent malignant glioma	Kunwar et al. (2000–2007)	IL13–PE38QQR	I II	Malignant glioma, grade III, IV	Completed	NCT00024570
Histologic effect/safety of pre/postoperative IL13-PE38QQR in recurrent resectable supratentorial malignant glioma patients	Kunwar et al. (2001–07)	IL13–PE38QQR	I	Malignant glioma, grade III, IV	Completed	NCT00024557
Phase IIb clinical trial with TGF-β2 antisense compound AP 12009 for recurrent or refractory high-grade glioma	Bogdahn et al. (2003–09)	TGF-β	II	Glioblastoma anaplastic astrocytoma	Completed	NCT00431561
Convection-enhanced delivery of paclitaxel for the treatment of recurrent malignant glioma: a Phase I/II clinical study	Ram et al. (2004)	Paclitaxel	I/II	Recurrent glioblastoma and anaplastic astrocytoma	Completed	NA
IL13-PE38QQR infusion after tumor resection, followed by radiation therapy with or without temozolomide in newly diagnosed malignant glioma	Kunwar et al. (2004–2007)	IL13–PE38QQR	I	Glioblastoma anaplastic astrocytoma oligoastrocytoma	Completed	NCT00089427
The PRECISE Trial: study of IL13-PE38QQR compared to GLIADEL wafer in patients with recurrent glioblastoma multiforme	Kunwar et al. (2004–07)	IL13–PE38QQR	III	Glioblastoma	Completed	NCT00076986
Safety and efficacy study to treat recurrent grade 4 malignant brain tumors	Kreitman et al. (2004–07)	TP-38	II	Glioblastoma	Completed	NCT00104091
Safety study of intracerebral topotecan for recurrent brain tumors	Bruce et al. (2004–11)	Topotecan	I II	Malignant glioma	Completed	NCT00308165
Study of immunotoxin, MR1–1	Bigner et al. (2006–12)	MR1–1KDEL	I	Supratentorial malignant brain tumor	Terminated	NCT01009866
Efficacy and Safety of AP 12009 in Patients With Recurrent or Refractory Anaplastic Astrocytoma or Secondary Glioblastoma (SAPPHIRE)	Del Maestro et al. (2008–14)	Trabedersen	III	Anaplastic astrocytoma glioblastoma	Terminated	NCT00761280
An open-label dose-escalation safety study of convection-enhanced delivery of IL13-PE38QQR in patients with progressive pediatric diffuse infiltrating brainstem glioma and supratentorial high-grade glioma	Heiss et al. (2009–present)	IL13–PE38QQR	I	Diffuse intrinsic pontine glioma high-grade glioma	Terminated	NCT00880061
Phase I study of cellular immunotherapy for recurrent/refractory malignant glioma using intratumoral infusions of GRm13Z40–2, an allogeneic $CD8^+$ cytolitic T-cell line…	Badie et al. (2010–13)	GRm13Z40–2 CTL	I	Brain tumors	Completed	NCT01082926
Safety Study of Replication-competent Adenovirus (Delta-24-rgd) in Patients With Recurrent Glioblastoma	Dirven et al. (2012–15)	Delta-24-RGD	I/II	Recurrent glioblastoma	Completed	NCT01582516
Poliovirus vaccine for recurrent glioblastoma multiforme (PVS-RIPO)	Friedman et al. (2012–present)	PSV-RIPO	I	Recurrent supratentorial glioblastoma multiforme glioblastoma	Recruiting	NCT01491893
Carboplatin in treating patients with recurrent high-grade gliomas	Elder et al. (2012–present)	Carboplatin	I	Anaplastic astrocytoma oligodendroglioma	Suspended	NCT01644955
Study of convection-enhanced, image-assisted delivery of liposomal-irinotecan in recurrent high-grade glioma	Butowski et al. (2014–present)	Nanoliposomal irinotecan	I	High-grade glioma	Enrollment by invitation	NCT02022644
	Zaghloul et al. (2015–present)	Muscimol	I	Parkinson's disease	Not yet recruiting	NCT00921128

Table 1 (continued)

Trial	Investigators (year)	Agent	Phase	Target disease	Current status	ClinicalTrials.gov identifier
Convection-Enhanced Delivery to Study the Pathophysiology Underlying the Clinical Features of Parkinson s Disease						
Topotecan Using Convection-Enhanced Delivery (CED) in High Grade Glioma	Vogelcaum et al. (2015–present)	Topotecan	0	High-grade glioma	Active, not recruiting	NCT02278510
Dose-escalation study of carboplatin administration into the brain for glioblastoma multiforme	Gill et al. (2015–present)	Carboplatin	I	Glioblastoma	Withdrawn	NCT01317212
Convection-Enhanced Delivery of 124I-8H9 for Patients With Non-Progressive Diffuse Pontine Gliomas Previously Treated With External Beam Radiation Therapy	Souweidane et al. (2016–present)	124I-8H9	I	Diffuse Intrinsic Pontine Glioma	Recruiting	NCT01502917
AAV2-GDNF for Advanced Parkinson s Disease	Heiss et al. (2016–present)	GDNF	I	Parkinson's disease	Recruiting	NCT01621581
D2C7 for Adult Patients With Recurrent Malignant Glioma	Bigner et al. (2016–present)	D2C7	I	Recurrent malignant glioma	Recruiting	NCT02303678
PVSRIPO for Recurrent Glioblastoma (GBM) (PVSRIPO)	Vlahovic et al. (2016–present)	PVSRIPO	I	Recurrent glioblastoma	Recruiting	NCT01491893

Trials summarized from ClinicalTrials.gov [65] and table adapted and modified with permission from *Future Medicine* [54]

NA = not applicable; TGF-β = transforming growth factor β

[68–74]. This study was highly influential, as it was the earliest demonstration of the safety and therapeutic efficacy of CED in a clinical setting. Eighteen patients with recurrent malignant tumors were treated, with 2 patients undergoing resection and thus being excluded from the trial, and 1 patient withdrawing from the trial. Of these remaining 15 patients, 9 had at least a 50% reduction in tumor volume when studied under magnetic resonance imaging (MRI). Additionally, toxicity was minimal, with only 3 patients (treated at higher concentrations) suffering peritumoral complications, and none of the patients suffering systemic toxicity [64].

PRECISE Trial

The only phase III trial using CED was the PRECISE trial (ClinicalTrials.gov identifier NCT00076986). This study, one of the largest using CED, was conducted after promising phase I studies [75]. The PRECISE trial compared survival in patients with recurrent GBM who were treated with CED of IL13–PE38QQR, a recombinant *Pseudomonas* exotoxin, (also known as cintredekin besudotox, or CB), to those treated with carmustine-impregnated wafers (Gliadel®), a current Food and Drug Administration-approved treatment for recurrent or newly diagnosed GBM. IL13–PE38QQR targets the interleukin-13 α-receptor, which is highly expressed in GBM [75–77], allowing for directed delivery of *Pseudomonas aeruginosa* exotoxin A. CED of IL13–PE38QQR was shown to be highly effective *in vitro*, providing a rationale for clinical testing [75, 78, 79].

The PRECISE study was designed to evaluate the efficacy of IL13–PE38QQR delivered by CED. Patients were randomized in a 2:1 manner to receive CED or the control therapy [80]. Unfortunately, this study did not demonstrate a survival benefit of patients treated with CB over the Gliadel® Wafers, as the median survival of the patients in the CED arm was 36.4 weeks *versus* 35.3 weeks for the patients enrolled in the control arm [11, 75]. However, the progression-free survival of this trial was 17.7 weeks *versus* 11.4 weeks in favor of CED [11]. Also, patients receiving CB had an increased rate of pulmonary embolism, which was attributed to longer hospitalizations [54, 81]. Many reasons for the trial's failure have been hypothesized. Eleven percent of the patients did not actually fulfill the inclusion criteria, and only 27% had complete resection [75]. Inaccurate catheter positioning may also have contributed to the unfavorable results, as only 49.8% of the catheters met all positioning criteria, and estimations of drug delivery to relevant target volumes correlated well with catheter positioning scores. As a result, the potential efficacy of the drugs delivered by CED may have been severely constrained by ineffective drug delivery [80]. The experience of the surgeon seemed to have a substantial effect on the efficacy of the intervention. Neurosurgeons who had previously treated at least 2 patients with a similar protocol had patients whose

overall survival was 19 weeks longer [33]. Finally, there was no real-time monitoring of drug distribution. Instead, catheter positioning scores and imaging change scores were used as surrogates. It should also be mentioned that the control performed much better than anticipated, as the median survival with GLIADEL® Wafers was 45 weeks, which is much higher than the 28-week median survival that had been reported previously [33].

Topotecan

Topotecan is a topoisomerase I inhibitor that causes single-stranded DNA breaks during DNA replication. It is an ideal agent for mitotically active targets in a quiescent environment [54, 82]. Systemic application of topotecan has been limited by poor BBB penetration, and phase II studies failed to show antitumor effects, while also showing severe side effects [54, 83]. Preclinical studies using CED with topotecan have shown promising results. In a rat study, CED of topotecan showed a significant survival advantage at concentrations less than those used systemically. This study showed that increased duration of therapy correlated with increased survival while avoiding adverse effects [54, 84]. A phase Ib dose-escalation study in patients with recurrent malignant gliomas, while not primarily designed to test treatment efficacy, demonstrated radiographic tumor regression in 69% of patients at nontoxic concentrations [10, 51]. This study also established a maximum tolerated dose for future phase II studies. Additionally, a follow-up study on the neurocognitive function and quality of life in these patients reported no severe detriment in either outcome [85].

Paclitaxel

A phase I/II study conducted in Israel demonstrated the antitumor potential of paclitaxel delivery using CED [86]. Paclitaxel (Taxol), has been demonstrated as an effective antitumor agent in a number of cancer types, including ovarian, breast, lung, head, and neck cancer [87]. It has also been demonstrated as effective against glioblastoma cells, both *in vitro* and *in vivo*, but unfortunately has demonstrated poor penetration across the BBB [88–91]. Paclitaxel functions by facilitating an aberrant microtubule assembly process that results in a microtubule complex that does not disassemble [92]. In this study, a response rate of 73% was observed, with 5/15 patients demonstrating complete responses and 6/15 demonstrating partial responses [86]. However, the investigators also reported significant complications, with a dose-dependent chemical meningitis being the most common side effect observed. Also observed was leakage of infusate into the CSF. In order to reduce the number of unwanted outcomes, future attempts should aim to optimize catheter placement using computer simulation software and real-time *in vivo* monitoring. To minimize complications from the agent itself, future attempts should consider adjust the dosage of paclitaxel or using a Cremophor-free paclitaxel preparation [86].

Diffuse Intrinsic Pontine Gliomas

Diffuse intrinsic pontine gliomas (DIPGs) comprise 75% to 80% of pediatric brainstem tumors, making them the most common brainstem tumors in children [93]. The location and pattern of these tumors precludes them from cytoreductive surgery, radiation has had poor success, and the relatively intact BBB and blood–tumor barrier make chemotherapy an ineffective option [93, 94]. DIPG are exceptionally lethal, with a median survival of approximately 1 year and a 2-year survival rate of < 20% [95, 96]. A variety of preclinical studies using CED for DIPG established its safety in the brainstem, as well as a 2012 study that demonstrated well-tolerated CED in 2 pediatric patients with DIPG [11, 97, 98]. There is currently 1 clinical trial investigating the use of CED in children with DIPG (ClinicalTrial.gov identifier NCT01502917), and it is currently in the recruiting phase. Like other studies, the major obstacle in studies for DIPG lies in the absence of a reliable method to determine *in vivo* drug distribution [53].

Poliovirus

Oncolytic viruses represent another promising area of cancer research that can be applied to CED. The ability of viruses to kill cancer cells has been recognized for nearly a century, but only in the past decade have clinical trials demonstrated a therapeutic benefit in patients [99–101, 102]. The virus carries out its antitumor effects in 2 ways. It transduces neoplastic cells and selectively replicates, thus causing direct lytic activity. In other cases, it can express a transgene that is toxic for the tumor cells, and in some cases, it can induce systemic antitumor immunity [101]. Currently, researchers at Duke University are conducting a phase I trial using CED of a recombinant, nonpathogenic poliovirus:rhinovirus chimera directly into tumor tissue [65]. Preliminary data have shown interesting results, with 3 patients remaining disease-free for 5 to 12 months post-treatment. However, other patients have had recurrent tumor growth after 2 months, and have had a decline in their condition [103].

Nontumor Clinical Trials

CED for Parkinson's Disease

Glial cell line-derived neurotrophic factor (GDNF) was first identified in 1993. It is glycosylated, disulfide-bonded homodimer protein that is one of the most powerful naturally

occurring human factors that enhances the survival of midbrain dopaminergic neurons [104, 105]. Studies in rat and monkey models from 1993 to 2000 showed that continuous delivery of GDNF at low levels was able to protect dopaminergic neurons from neurotoxin-induced cell death. These studies also showed improvement in motor function and a decrease in Parkinsonian symptoms [105]. However, GDNF penetration into brain tissue was limited, and in 2003, Gill et al. [106] initiated a phase I safety trial, using direct intraparenchymal GDNF delivery into the putamen of 5 patients with Parkinson's disease. While only a phase I trial, it suggested a direct effect of GDNF on dopamine function, with a 39% improvement in off-medication motor function, 61% improvement in daily activity, and a 64% decrease in medication-induced dyskinesias. Amgen initiated a "double-blind" trial later in 2003 with 34 patients. Preliminary data did not show any clinical improvement, and later, in 2004, Amgen halted the study as it detected cerebellar neuronal loss and the presence of "neutralizing antibodies" in 2 study participants [105]. Adequate delivery failure has been proposed for the failure of the phase II trial. The failure in delivery was perhaps caused by the use of backflow-prone catheters, and a suboptimal delivery protocol [33, 107, 108]. There is currently a phase Ib dose escalation trial (ClinicalTrials.gov identifier NCT01621581) designed to test the safety and effectiveness of CED of adeno-associated virus encoding GDNF in patients with advanced Parkinson's disease.

Also attempted was the use of neurturin, a growth factor delivered via an adeno-associated viral vector carrier. Preclinical trials showed promising results, where the virus was injected into the putamen and was transported to the substantia nigra [33, 109]. A combined phase II/phase III trial failed, and in these trials there was a failure to reach the substantia nigra [33, 110]. A subsequent trial that attempted to deliver the vector to both the putamen and the substantia nigra also failed [33, 111]. Many reasons have been proposed for this study's failure, including the lack of intraoperative MRI techniques and the need to recruit patients at an earlier stage in their disease [112].

The important lessons that should be learned from these clinical trials follow. 1) Clinical trials with should focus on infusion catheter optimization, as well as improved catheter placement. An experienced surgical team is desirable to ensure optimal catheter placement and patient selection. 2) The protocol should be flexible enough to adjust for parameters like flow rate and duration of infusion on a case-by-case basis. 3) A uniform method to ensure exact and reproducible drug delivery should apply. Verification of drug delivery, and the use of *in vivo* monitoring of drug distribution whether it be via co-infusion of tracers that can be imaged, or by other means, are both necessary to improve the delivery and efficacy of therapeutic agents [11, 80]. In many studies, the failure of the delivery technique is mistaken for a failure of the therapy. If we are to truly assess the effectiveness of a therapeutic agent, patients who underwent effective delivery could be postselected in the statistical analysis, thus isolating the efficacy of the therapy from the delivery technique [33]. 4) Future trials should use more rigorous inclusion criteria based on tumor molecular biology, particularly when drugs are specific to tumor targets [11, 75].

Future Improvements in the Technique

New-Generation Catheters

Reflux-Preventing Catheters

Backflow, or reflux, is an unintended and detrimental phenomenon that can occur during CED. Not only does reflux decrease the volume and predictability of drug distribution, but it can lead to leakage into unintended areas of the brain and possibly lead to excess toxicity. Experimental results have demonstrated that CED using catheters with larger diameters is more likely to lead to reflux [113–115]. This observation lead to the step-down catheter design [50]. The catheter developed by Fiandaca et al. [38] allows for flow rates up to 5.0 μl/min without ensuing reflux. In this catheter design, the cannula extends beyond the end of the needle by 5 to 10 mm. Unfortunately, in 20% of catheter placements, reflux can still be seen, but often at higher infusion rates [113].

Multiple-Hole/Hollow-Fiber Catheters

Originally, catheters used for CED were multiport catheters that were designed for ventricular shunts in situations of hydrocephalus. Multiple port catheters provide an appealing delivery mechanism, as the multiple ports may provide better pressure output, thus improving the volume of distribution achieved [11]. However, an obstacle in the successful usage of multiport catheters CED is obtaining predictable flows from all of the ports. Very often, the infusate flows only through the most proximal port, making flow unpredictable and the remaining ports effectively useless. Possible solutions to this problem include increasing resistance inside the catheter with a porous material, creating catheters with several separate lumens within a single catheter body with each lumen feeding its own port, devising a catheter with controllable portholes, actively controlling the substance once it has been pumped, and, most simply, using a catheter with a single end port [16]. Most recently, a hollow-fiber catheter with multiple ports has been developed by TwinStar Medical (Saint Paul, MN, USA) to address these issues [50]. The hollow fiber contains millions of openings along its wall (Fig. 4). These openings are extremely small, on the order of 0.45 μm [113].

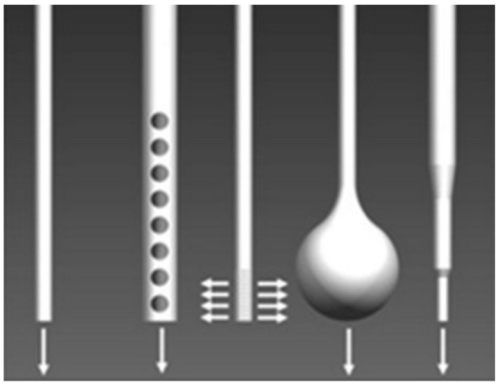

Fig. 4 The different designs of catheters used in convection-enhanced delivery. From left to right they are end port cannula, multiport cannula, porous-tipped catheter, balloon-tipped catheter, and stepped-profile catheter. Figure reprinted from Lewis et al. [113]

These catheters have shown promising results, increasing the amount of infusate transferred by up to 3-fold, improving the uniformity of distribution, and reducing backflow [50, 116]. In addition, the hollow-fiber catheter should avoid clogging. A combination of the step design and porous wall designs has been proposed to reduce backflow [11].

Ultrafine Catheters

Renishaw (Wotton-under-Edge, UK) has developed ultrafine, tissue-compatible, antireflux catheters, which produce minimal tissue damage. The use of these catheters, which would require the assistance of a guidance sheath, overcomes the issues traditionally associated with small catheters, such as floppiness, and allows for accurate placement, as well as backflow resistance. In addition, as many catheters may potentially be used, this technique could be used as a method of conforming the drug delivery to the shape that best suits the relevant anatomy [50].

Balloon-Tipped Catheter

This approach involves the use of a balloon proximal to the catheter tip. This balloon can fill the resection cavity, thus forcing infusate into the cavity and away from the catheter tip and therefore limiting reflux. Studies using this technique on canine models have demonstrated extensive delivery of infusate, and further studies need to be performed to examine the efficacy of this promising technique [113, 117, 118].

Prolonged Delivery Via Subcutaneous Implantation

The use of externalized catheters is associated with an increased risk of infection as therapy length increases, thus shortening the therapy length [51]. However, studies have shown a therapeutic benefit from the prolonged delivery of agent [10]. For this reason, a method that achieves both prolonged delivery, as well as safety, has been employed. Sonabend et al. [119] examined prolonged delivery of topotecan using a subcutaneous pump in a pig model, and were able to show a number of promising results. This study demonstrated that prolonged delivery was well tolerated, and topotecan maintained bioactivity up to 10 days after infusion at body temperature. The study also demonstrated that prolonged CED leads to a sustained volume of distribution (Fig. 5) [119]. This approach shows great potential, as it allows for constant regional infusion of agents in an outpatient setting [119].

Modeling

CED studies, while displaying extensive and relatively homogenous distributions of target agents, have also displayed variability in the spatial distribution from patient to patient [60]. There is also a degree of unpredictability to the geometry of the distribution. These factors present an obstacle in ensuring sufficient drug delivery to the areas of interest [60]. There is currently a Food and Drug Administration-approved software, developed by BrainLAB, which uses the input of MRI-obtained data to calculate the desired drug distribution volume and a 3-dimensional visualization of the plan of treatment, including the number and position of catheters (Fig. 6) [60, 113]. This approach accounts for anatomical and physiological variability, which have been shown to play a major role in drug distribution [50]. A study by Sampson et al. [60] that retrospectively examined data from the PRECISE trial demonstrated that the use of this simulation algorithm was considered clinically useful for 84.6% of the catheters simulated after placement, and illustrates the promise associated with software modeling before CED [50]. As imaging technology improves, the input to the software will be more accurate, thus producing more accurate and clinically useful simulations.

Imaging

While CED, in theory, is a promising delivery technique, in actuality its efficacy is entirely dependent on mechanical constraints related to particular anatomic considerations for a given patient. Many clinical trials have failed, presumably owing to poor convection. Yet, a major challenge for the optimization of CED, and the investigation of whether or not efficacy of the treatments was limited by poor delivery, is the lack of ability to monitor and confirm adequate *in vivo* drug distribution [34]. This has led the possibility of discarding potentially beneficial agents as useless [11, 60, 120]. There is a need to monitor the tissue concentration of a given particle *in vivo*. Monitoring can generally be performed in 2 ways: directly or indirectly. The direct method entails either labeling the molecule itself with a detectable radioisotope, or by using a

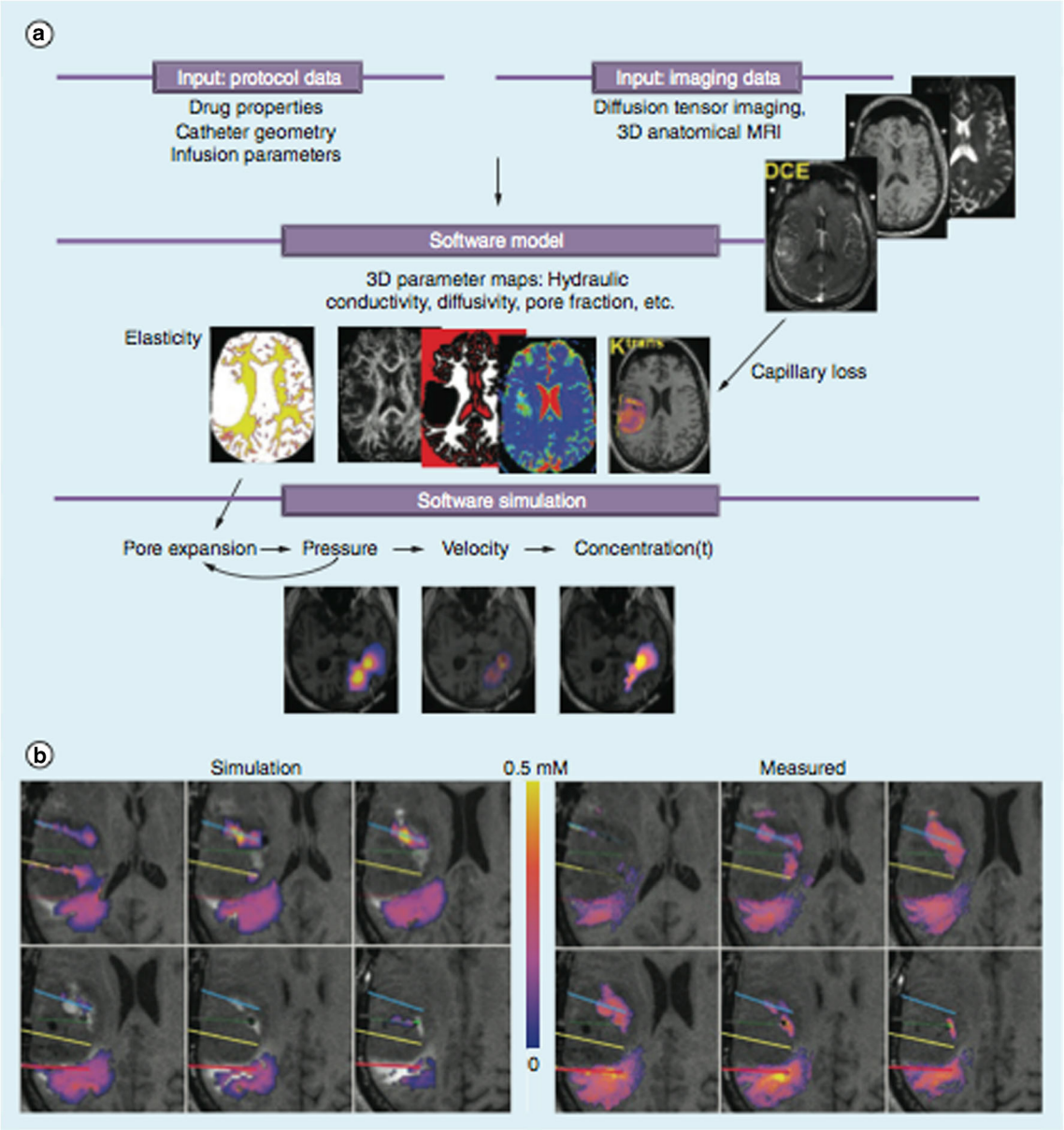

Fig. 5 Illustration of the advantage conferred by prolonged infusions of topotecan-gadolinium using a subcutaneous pump. The graph compares the changes in relative volume in 10-day infusions to 3-day infusions. In both scenarios, a peak is observed approximately 2 to 3 days after infusion, after which the 3-day infusion begins to trend downwards and the 10-day infusion hovered around its peak value. Figure reprinted with permission from Oxford University Press [119]

surrogate tracer that approximates the distribution patterns of the therapy. The former technique is expensive and not frequently performed [33].

Currently, many monitoring techniques rely on the alterations of radiographic appearance as a result of fluid administration or drug-induced effects on tissue [36]. However, this is subject to limitations and going forward, more accurate methods will be required. Examples of existing imaging techniques include albumin-conjugated surrogate tracers, T2-weighted MRI changes, gadolinium-based liposome constructs, gadolinium-bound albumin, and gadolinium direct infusion [36]. An elaboration on a few of these follows.

Albumin and Gadolinium-Diethylenetriaminepentaacetic Acid CED-infused albumin tracers can be linked to gadolinium-diethylenetriaminepentaacetic acid (Gd-DPTA), which can then be visualized with traditional imaging techniques [120]. Albumin is used because of its hydrophilicity and its similarity in size and shape to the protein toxin used in the treatment of recurrent GBM [33]. Gd-DTPA is often used a surrogate tracer, as it is widely available owing to its use as an MRI contrast agent. Attempts to incorporate Gd-DTPA into impregnated liposomes have been made, but owing to manufacturing difficulties this may not be the most feasible approach [120, 121]. Gd-DTPA has been used in a variety of

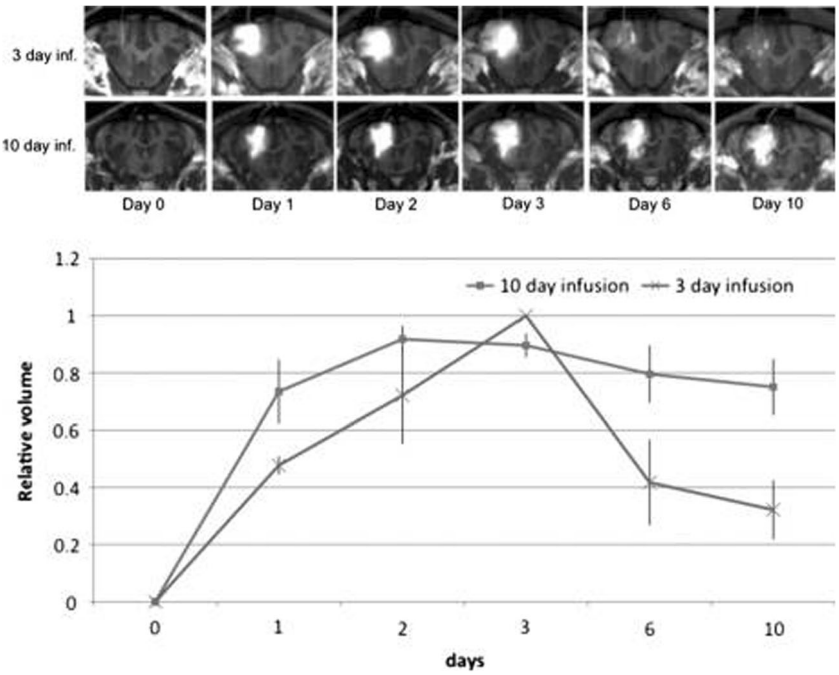

Fig. 6 Schematic summarizing the modeling process described in the review. (A) The software requires protocol, and imaging data generates a simulation of fluid and molecular transport. The simulation also allows for interstitial expansion and compromised blood–brain barrier. (B) The simulated and measured distributions of Magnevist™ are compared across six axial slices, with each slice being taken 5 mm apart. Units for concentration color mmol of agent/l of solution. Figure reprinted with permission from *Therapeutic Delivery* [33]

proprietary formulations such as Magnevist, Omniscan, or Prohance [120]. With these formulations, the distribution is often indicated by a certain threshold intensity on T1-weighted MRI. However, this has its limitations and is generally not preferred over quantitative methods of determining concentration and distribution [34]. These quantitative methods have been developed, now allowing for the determination of tracer concentrations [122–125].

MRI T2 Imaging Changes Using MRI signal changes as an estimate of CED infusate distribution has been suggested in a number of preclinical models [86, 120, 123, 126]. In addition, this has been supported by more recent clinical evidence, as Sampson et al. [127] have shown that intraparenchymal drug coverage can be predicted using T2-weighted MRI changes in combination with single-photon emission computed tomography imaging. This also applies in situations of pre-existing T2 MRI hyperintensity [120].

Conclusion

CED is a promising technique that can potentially overcome limitations of systemic delivery. Successful clinical translation of this technique could be applicable to a variety of CNS disorders that until now have proved elusive, and could potentially close the gap between therapeutic advancements and the prognoses for various neurological illnesses. However, developments in *in vivo* monitoring, simulations, catheter technology, prolonged delivery, and other facets of CED need to take place before CED can reach its full therapeutic potential. Given the number of clinical trials investigating CED currently active, it is likely that major developments surrounding this technique will occur in the relatively near future.

Acknowledgements This work was supported by National Institutes of Health (NIH) grant T35 AG044303 (A.M.M.), the NIH Office of the Director 1DP5OD021356-01 (A.M.S.) and R01 CA161404 (J.N.B.).

References

1. Kanu OO, Mehta A, Di C, et al. Glioblastoma multiforme: a review of therapeutic targets. Expert Opin Ther Targets 2009;13:701–718.
2. Ostrom QT, Gittleman H, Farah P, et al. CBTRUS statistical report: Primary brain and central nervous system tumors diagnosed in the United States in 2006–2010. Neuro Oncol 2013;15(Suppl. 2):ii1-56.
3. Stupp R, Mason WP, van den Bent MJ, et al. Radiotherapy plus concomitant and adjuvant temozolomide for glioblastoma. N Engl J Med 2005;352:987–996.
4. Stupp R, Hegi ME, Mason WP, et al. Effects of radiotherapy with concomitant and adjuvant temozolomide versus radiotherapy alone on survival in glioblastoma in a randomised phase III study: 5-year analysis of the EORTC-NCIC trial. Lancet Oncol 2009;10:459–466.
5. Blasberg RG, Patlak C, Fenstermacher JD. Intrathecal chemotherapy: brain tissue profiles after ventriculocisternal perfusion. J Pharmacol Exp Ther 1975;195:73–83.
6. Chen PY, Ozawa T, Drummond DC, et al. Comparing routes of delivery for nanoliposomal irinotecan shows superior anti-tumor activity of local administration in treating intracranial glioblastoma xenografts. Neuro Oncol 2013;15:189–197.

7. Langer R. New methods of drug delivery. Science 1990;249: 1527–1533.
8. Pardridge WM. Drug delivery to the brain. J Cereb Blood Flow Metab 1997;17:713–731.
9. Lesniak MS, Brem H. Targeted therapy for brain tumours. Nat Rev Drug Discov 2004;3:499–508.
10. Yun J, Rothrock RJ, Canoll P, Bruce JN. Convection-enhanced delivery for targeted delivery of antiglioma agents: the translational experience. J Drug Deliv 2013;2013:107573.
11. Zhou Z, Singh R, Souweidane MM. Convection-enhanced delivery in diffuse intrinsic pontine glioma. Curr Neuopharmacol 2017;15:116–128.
12. Bobo RH, Laske DW, Akbasak A, Morrison PF, Dedrick RL, Oldfield EH. Convection-enhanced delivery of macromolecules in the brain. Proc Natl Acad Sci U S A 1994;91:2076–2080.
13. Morrison PF, Laske DW, Bobo H, Oldfield EH, Dedrick RL. High-flow microinfusion: tissue penetration and pharmacodynamics. Am J Physiol 1994;266:R292-305.
14. Lonser RR, Walbridge S, Garmestani K, et al. Successful and safe perfusion of the primate brainstem: in vivo magnetic resonance imaging of macromolecular distribution during infusion. J Neurosurg 2002;97:905–913.
15. Nguyen TT, Pannu YS, Sung C, et al. Convective distribution of macromolecules in the primate brain demonstrated using computerized tomography and magnetic resonance imaging. J Neurosurg 2003;98:584–590.
16. Raghavan R, Brady ML, Rodriguez-Ponce MI, Hartlep A, Pedain C, Sampson JH. Convection-enhanced delivery of therapeutics for brain disease, and its optimization. Neurosurg Focus 2006;20: E12.
17. Corem-Salkmon E, Ram Z, Daniels D, et al. Convection-enhanced delivery of methotrexate-loaded maghemite nanoparticles. Int J Nanomedicine 2011;6:1595–1602.
18. Lonser RR, Sarntinoranont M, Morrison PF, Oldfield EH. Convection-enhanced delivery to the central nervous system. J Neurosurg 2015;122:697–706.
19. Heiss JD, Walbridge S, Morrison P, et al. Local distribution and toxicity of prolonged hippocampal infusion of muscimol. J Neurosurg 2005;103:1035–1045.
20. Lieberman DM, Laske DW, Morrison PF, Bankiewicz KS, Oldfield EH. Convection-enhanced distribution of large molecules in gray matter during interstitial drug infusion. J Neurosurg 1995;82:1021–1029.
21. Lonser RR, Corthesy ME, Morrison PF, Gogate N, Oldfield EH. Convection-enhanced selective excitotoxic ablation of the neurons of the globus pallidus internus for treatment of parkinsonism in nonhuman primates. J Neurosurg 1999;91:294–302.
22. Ciesielska A, Mittermeyer G, Hadaczek P, Kells AP, Forsayeth J, Bankiewicz KS. Anterograde axonal transport of AAV2-GDNF in rat basal ganglia. Mol Ther 2011;19:922–927.
23. Kells AP, Hadaczek P, Yin D, et al. Efficient gene therapy-based method for the delivery of therapeutics to primate cortex. Proc Natl Acad Sci U S A 2009;106:2407–2411.
24. Ksendzovsky A, Walbridge S, Saunders RC, Asthagiri AR, Heiss JD, Lonser RR. Convection-enhanced delivery of M13 bacteriophage to the brain. J Neurosurg 2012;117:197–203.
25. Barker FG, 2nd, Chang SM, Gutin PH, et al. Survival and functional status after resection of recurrent glioblastoma multiforme. Neurosurgery 1998;42:709–720.
26. Lonser RR, Gogate N, Morrison PF, Wood JD, Oldfield EH. Direct convective delivery of macromolecules to the spinal cord. J Neurosurg 1998;89:616–622.
27. Lonser RR, Weil RJ, Morrison PF, Governale LS, Oldfield EH. Direct convective delivery of macromolecules to peripheral nerves. J Neurosurg 1998;89:610–615.
28. Murad GJ, Walbridge S, Morrison PF, et al. Image-guided convection-enhanced delivery of gemcitabine to the brainstem. J Neurosurg 2007;106:351–356.
29. Asthagiri AR, Walbridge S, Heiss JD, Lonser RR. Effect of concentration on the accuracy of convective imaging distribution of a gadolinium-based surrogate tracer. J Neurosurg 2011;115:467–473.
30. Dickinson PJ, LeCouteur RA, Higgins RJ, et al. Canine model of convection-enhanced delivery of liposomes containing CPT-11 monitored with real-time magnetic resonance imaging: laboratory investigation. J Neurosurg 2008;108:989–998.
31. Huynh NT, Passirani C, Allard-Vannier E, et al. Administration-dependent efficacy of ferrociphenol lipid nanocapsules for the treatment of intracranial 9L rat gliosarcoma. Int J Pharm 2012;423:55–62.
32. Szerlip NJ, Walbridge S, Yang L, et al. Real-time imaging of convection-enhanced delivery of viruses and virus-sized particles. J Neurosurg 2007;107:560–567.
33. Raghavan R, Brady, M. Sampson, JH. Delivering therapy to target: improving the odds for successful drug development. Ther Deliv 2016;7:457–481.
34. Sampson JH, Raghavan R, Brady M, Friedman AH, Bigner D. Convection-enhanced delivery. J Neurosurg 2011;115:463–464.
35. Reardon DA, Rich JN, Friedman HS, Bigner DD. Recent advances in the treatment of malignant astrocytoma. J Clin Oncol 2006;24:1253–1265.
36. Mehta AI, Choi BD, Raghavan R, et al. Imaging of convection enhanced delivery of toxins in humans. Toxins (Basel) 2011;3: 201–206.
37. Healy AT, Vogelbaum MA. Convection-enhanced drug delivery for gliomas. Surg Neurol Int 2015;6(Suppl. 1):S59-S67.
38. Fiandaca MS, Forsayeth JR, Dickinson PJ, Bankiewicz KS. Image-guided convection-enhanced delivery platform in the treatment of neurological diseases. Neurotherapeutics 2008;5:123–127.
39. Casanova F, Carney PR, Sarntinoranont M. Effect of needle insertion speed on tissue injury, stress, and backflow distribution for convection-enhanced delivery in the rat brain. *PLOS ONE* 2014;9: e94919.
40. Sillay KA, McClatchy SG, Shepherd BA, Venable GT, Fuehrer TS. Image-guided convection-enhanced delivery into agarose gel models of the brain. J Vis Exp 2014(87).
41. Krauze MT, Saito R, Noble C, Tamas M, Bringas J, Park JW, et al. Reflux-free cannula for convection-enhanced high-speed delivery of therapeutic agents. J Neurosurg 2005;103:923–929.
42. Allard E, Passirani C, Benoit JP. Convection-enhanced delivery of nanocarriers for the treatment of brain tumors. Biomaterials 2009;30:2302–2318.
43. Jain RK. Physiological barriers to delivery of monoclonal antibodies and other macromolecules in tumors. Cancer Res 1990;50(3 Suppl.):814s-819s.
44. Jain RK. Transport of molecules in the tumor interstitium: a review. Cancer Res 1987;47:3039–3051.
45. Jain RK. Transport of molecules across tumor vasculature. Cancer Metastasis Rev 1987;6:559–593.
46. Jain RK. Tumor physiology and antibody delivery. Front Radiat Ther Oncol 1990;24:32–46.
47. Jain RK. Vascular and interstitial barriers to delivery of therapeutic agents in tumors. Cancer Metastasis Rev 1990;9:253–266.
48. Jain RK, Baxter LT. Mechanisms of heterogeneous distribution of monoclonal antibodies and other macromolecules in tumors: significance of elevated interstitial pressure. Cancer Res 1988;48:7022–7032.
49. Brady ML, Raghavan R, Alexander A, Kubota K, Sillay K, Emborg ME. Pathways of infusate loss during convection-enhanced delivery into the putamen nucleus. Stereotact Funct Neurosurg 2013;91:69–78.

50. Bidros DS, Liu JK, Vogelbaum MA. Future of convection-enhanced delivery in the treatment of brain tumors. Future Oncol 2010;6:117–125.
51. Bruce JN, Fine RL, Canoll P, et al. Regression of recurrent malignant gliomas with convection-enhanced delivery of topotecan. Neurosurgery 2011;69:1272–1279.
52. Patel SJ, Shapiro WR, Laske DW, Jensen RL, Asher AL, Wessels BW, et al. Safety and feasibility of convection-enhanced delivery of Cotara for the treatment of malignant glioma: initial experience in 51 patients. Neurosurgery 2005;56:1243–1252.
53. Souweidane MM. Editorial: convection-enhanced delivery for diffuse intrinsic pontine glioma. J Neurosurg Pediatr 2014;13:273–274.
54. Ung TH, Malone H, Canoll P, Bruce JN. Convection-enhanced delivery for glioblastoma: targeted delivery of antitumor therapeutics. CNS Oncol 2015;4:225–234.
55. Hadaczek P, Kohutnicka M, Krauze MT, et al. Convection-enhanced delivery of adeno-associated virus type 2 (AAV2) into the striatum and transport of AAV2 within monkey brain. Hum Gene Ther 2006;17:291–302.
56. Krauze MT, Forsayeth J, Yin D, Bankiewicz KS. Convection-enhanced delivery of liposomes to primate brain. Methods Enzymol 2009;465:349–362.
57. Sampson JH, Brady ML, Petry NA, et al. Intracerebral infusate distribution by convection-enhanced delivery in humans with malignant gliomas: descriptive effects of target anatomy and catheter positioning. Neurosurgery 2007;60(2 Suppl. 1):ONS89-98.
58. Vavra M, Ali MJ, Kang EW, et al. Comparative pharmacokinetics of 14C-sucrose in RG-2 rat gliomas after intravenous and convection-enhanced delivery. Neuro Oncol 2004;6:104–112.
59. Geer CP, Grossman SA. Interstitial fluid flow along white matter tracts: a potentially important mechanism for the dissemination of primary brain tumors. J Neurooncol 1997;32:193–201.
60. Sampson JH, Raghavan R, Brady ML, et al. Clinical utility of a patient-specific algorithm for simulating intracerebral drug infusions. Neuro Oncol 2007;9:343–353.
61. Voges J, Reszka R, Gossmann A, et al. Imaging-guided convection-enhanced delivery and gene therapy of glioblastoma. Ann Neurol 2003;54:479–487.
62. Linninger AA, Somayaji MR, Mekarski M, Zhang L. Prediction of convection-enhanced drug delivery to the human brain. J Theor Biol 2008;250:125–138.
63. Lonser RR, Warren KE, Butman JA, et al. Real-time image-guided direct convective perfusion of intrinsic brainstem lesions. Technical note. J Neurosurg 2007;107:190–197.
64. Laske DW, Youle RJ, Oldfield EH. Tumor regression with regional distribution of the targeted toxin TF-CRM107 in patients with malignant brain tumors. Nat Med 1997;3:1362–1368.
65. Bigner DD. PVSRIPO for Recurrent Glioblastoma (GBM) (PVSRIPO). NCT01491893. Available from: https://clinicaltrials.gov/ct2/show/NCT01491893.
66. Greenfield L, Johnson VG, Youle RJ. Mutations in diphtheria toxin separate binding from entry and amplify immunotoxin selectivity. Science 1987;238:536–539.
67. Johnson VG, Wrobel C, Wilson D, et al. Improved tumor-specific immunotoxins in the treatment of CNS and leptomeningeal neoplasia. J Neurosurg 1989;70:240–248.
68. Larrick JW, Cresswell P. Modulation of cell surface iron transferrin receptors by cellular density and state of activation. J Supramol Struct 1979;11:579–586.
69. Faulk WP, Hsi BL, Stevens PJ. Transferrin and transferrin receptors in carcinoma of the breast. Lancet 1980;2:390–392.
70. Trowbridge IS, Omary MB. Human cell surface glycoprotein related to cell proliferation is the receptor for transferrin. Proc Natl Acad Sci U S A 1981;78:3039–3043.
71. Shindelman JE, Ortmeyer AE, Sussman HH. Demonstration of the transferrin receptor in human breast cancer tissue. Potential marker for identifying dividing cells. Int J Cancer 1981;27:329–334.
72. Klausner RD, Van Renswoude J, Ashwell G, et al. Receptor-mediated endocytosis of transferrin in K562 cells. J Biol Chem 1983;258:4715–4724.
73. Prior R, Reifenberger G, Wechsler W. Transferrin receptor expression in tumours of the human nervous system: relation to tumour type, grading and tumour growth fraction. Virchows Arch A Pathol Anat Histopathol 1990;416:491–496.
74. Gatter KC, Brown G, Trowbridge IS, Woolston RE, Mason DY. Transferrin receptors in human tissues: their distribution and possible clinical relevance. J Clin Pathol 1983;36:539–545.
75. Mueller S, Polley MY, Lee B, et al. Effect of imaging and catheter characteristics on clinical outcome for patients in the PRECISE study. J Neurooncol 2011;101:267–277.
76. Joshi BH, Plautz GE, Puri RK. Interleukin-13 receptor alpha chain: a novel tumor-associated transmembrane protein in primary explants of human malignant gliomas. Cancer Res 2000;60:1168–1172.
77. Liu H, Jacobs BS, Liu J, et al. Interleukin-13 sensitivity and receptor phenotypes of human glial cell lines: non-neoplastic glia and low-grade astrocytoma differ from malignant glioma. Cancer Immunol Immunother 2000;49:319–324.
78. Debinski W, Obiri NI, Pastan I, Puri RK. A novel chimeric protein composed of interleukin 13 and Pseudomonas exotoxin is highly cytotoxic to human carcinoma cells expressing receptors for interleukin 13 and interleukin 4. J Biol Chem 1995;270:16775–16780.
79. Husain SR, Joshi BH, Puri RK. Interleukin-13 receptor as a unique target for anti-glioblastoma therapy. Int J Cancer 2001;92:168–175.
80. Sampson JH, Archer G, Pedain C, et al. Poor drug distribution as a possible explanation for the results of the PRECISE trial. J Neurosurg 2010;113:301–309.
81. Kunwar S, Prados MD, Chang SM, et al. Direct intracerebral delivery of cintredekin besudotox (IL13-PE38QQR) in recurrent malignant glioma: a report by the Cintredekin Besudotox Intraparenchymal Study Group. J Clin Oncol 2007;25:837–844.
82. Pommier Y. Topoisomerase I inhibitors: camptothecins and beyond. Nat Rev Cancer 2006;6:789–802.
83. Burch PA, Bernath AM, Cascino TL, et al. A North Central Cancer Treatment Group phase II trial of topotecan in relapsed gliomas. Invest New Drugs 2000;18:275–280.
84. Lopez KA, Tannenbaum AM, Assanah MC, et al. Convection-enhanced delivery of topotecan into a PDGF-driven model of glioblastoma prolongs survival and ablates both tumor-initiating cells and recruited glial progenitors. Cancer Res 2011;71:3963–3971.
85. Oberg JA, Dave AN, Bruce JN, Sands SA. Neurocognitive functioning and quality of life in patients with recurrent malignant gliomas treated on a phase Ib trial evaluating topotecan by convection-enhanced delivery. Neurooncol Pract 2014;1:94–100.
86. Lidar Z, Mardor Y, Jonas T, et al. Convection-enhanced delivery of paclitaxel for the treatment of recurrent malignant glioma: a phase I/II clinical study. J Neurosurg 2004;100:472–479.
87. Cheson BD. Clinical trials referral resource. Update on taxol trials. Oncology (Williston Park) 1993;7:63.
88. Terzis AJ, Thorsen F, Heese O, et al. Proliferation, migration and invasion of human glioma cells exposed to paclitaxel (Taxol) in vitro. Br J Cancer 1997;75:1744–1752.
89. Monk BJ, Walker JL, Tewari K, Ramsinghani NS, Nisar Syed AM, DiSaia PJ. Open interstitial brachytherapy for the treatment of local-regional recurrences of uterine corpus and cervix cancer after primary surgery. Gynecol Oncol 1994;52:222–228.

90. Chang MY, Soong YK, Huang CC. Comparison of histocompatibility between couples with idiopathic recurrent spontaneous abortion and normal multipara. J Formos Med Assoc 1991;90:153–159.
91. Fetell MR, Grossman SA, Fisher JD, et al. Preirradiation paclitaxel in glioblastoma multiforme: efficacy, pharmacology, and drug interactions. New Approaches to Brain Tumor Therapy Central Nervous System Consortium. J Clin Oncol 1997;15:3121–3128.
92. Jordan MA, Toso RJ, Thrower D, Wilson L. Mechanism of mitotic block and inhibition of cell proliferation by taxol at low concentrations. Proc Natl Acad Sci U S A 1993;90:9552–9556.
93. Warren KE. Diffuse intrinsic pontine glioma: poised for progress. Front Oncol 2012;2:205.
94. Occhiogrosso G, Edgar MA, Sandberg DI, Souweidane MM. Prolonged convection-enhanced delivery into the rat brainstem. Neurosurgery 2003;52:388–393.
95. Frazier JL, Lee J, Thomale UW, Noggle JC, Cohen KJ, Jallo GI. Treatment of diffuse intrinsic brainstem gliomas: failed approaches and future strategies. J Neurosurg Pediatr 2009;3:259–269.
96. Khatua S, Moore KR, Vats TS, Kestle JR. Diffuse intrinsic pontine glioma-current status and future strategies. Childs Nerv Syst 2011;27:1391–1397.
97. Sandberg DI, Edgar MA, Souweidane MM. Convection-enhanced delivery into the rat brainstem. J Neurosurg 2002;96:885–891.
98. Anderson RC, Kennedy B, Yanes CL, et al. Convection-enhanced delivery of topotecan into diffuse intrinsic brainstem tumors in children. J Neurosurg Pediatr 2013;11:289–295.
99. Moore AE. Effect of inoculation of the viruses of influenza A and herpes simplex on the growth of transplantable tumors in mice. Cancer 1949;2:516–524.
100. Andtbacka RH, Kaufman HL, Collichio F, et al. Talimogene laherparepvec improves durable response rate in patients with advanced melanoma. J Clin Oncol 2015;33:2780–2788.
101. Kaufman HL, Kohlhapp FJ, Zloza A. Oncolytic viruses: a new class of immunotherapy drugs. Nat Rev Drug Discov 2015;14:642–662.
102. Moore AE. The destructive effect of the virus of Russian Far East encephalitis on the transplantable mouse sarcoma 180. Cancer 1949;2:525–534.
103. Duke Today. Poliovirus vaccine trial shows early promise for recurrent glioblastoma. Medicine, Academics, Research. Available at: https://today.duke.edu/2013/07/poliovirus-vaccine-trial-shows-promise-recurrent-glioblastoma. Accessed February 26, 2017.
104. Lin LF, Doherty DH, Lile JD, Bektesh S, Collins F. GDNF: a glial cell line-derived neurotrophic factor for midbrain dopaminergic neurons. Science 1993;260:1130–1132.
105. Background Information on GDNF – a timeline: Parkinson's Disease Foundation. Available at: http://www.pdf.org/en/science_news/release/pr_1216665220. Accessed June 26, 2016.
106. Gill SS, Patel NK, Hotton GR, et al. Direct brain infusion of glial cell line-derived neurotrophic factor in Parkinson disease. Nat Med 2003;9:589–595.
107. Salvatore MF, Ai Y, Fischer B, et al. Point source concentration of GDNF may explain failure of phase II clinical trial. Exp Neurol 2006;202:497–505.
108. Morrison PF, Lonser RR, Oldfield EH. Convective delivery of glial cell line-derived neurotrophic factor in the human putamen. J Neurosurg 2007;107:74–83.
109. Bartus RT, Herzog CD, Bishop K, et al. Issues regarding gene therapy products for Parkinson's disease: the development of CERE-120 (AAV-NTN) as one reference point. Parkinsonism Relat Disord 2007;13(Suppl. 3):S469-S477.
110. Olanow CW, Kieburtz K, Schapira AH. Why have we failed to achieve neuroprotection in Parkinson's disease? Ann Neurol 2008;64(Suppl. 2):S101-S110.
111. Bartus RT, Weinberg MS, Samulski RJ. Parkinson's disease gene therapy: success by design meets failure by efficacy. Mol Ther 2014;22:487–497.
112. Warren Olanow C, Bartus RT, Baumann TL, et al. Gene delivery of neurturin to putamen and substantia nigra in Parkinson disease: a double-blind, randomized, controlled trial. Ann Neurol 2015;78:248–257.
113. Debinski W, Tatter SB. Convection-enhanced delivery for the treatment of brain tumors. Expert Rev Neurother 2009;9:1519–1527.
114. Chen MY, Lonser RR, Morrison PF, Governale LS, Oldfield EH. Variables affecting convection-enhanced delivery to the striatum: a systematic examination of rate of infusion, cannula size, infusate concentration, and tissue-cannula sealing time. J Neurosurg 1999;90:315–320.
115. Morrison PF, Chen MY, Chadwick RS, Lonser RR, Oldfield EH. Focal delivery during direct infusion to brain: role of flow rate, catheter diameter, and tissue mechanics. Am J Physiol 1999;277:R1218-R1229.
116. Oh S, Odland R, Wilson SR, et al. Improved distribution of small molecules and viral vectors in the murine brain using a hollow fiber catheter. J Neurosurg 2007;107:568–577.
117. Olson JJ, Zhang Z, Dillehay D, Stubbs J. Assessment of a balloon-tipped catheter modified for intracerebral convection-enhanced delivery. J Neurooncol 2008;89:159–168.
118. Olivi A, Grossman SA, Tatter S, et al. Dose escalation of carmustine in surgically implanted polymers in patients with recurrent malignant glioma: a New Approaches to Brain Tumor Therapy CNS Consortium trial. J Clin Oncol 2003;21:1845–1849.
119. Sonabend AM, Stuart RM, Yun J, et al. Prolonged intracerebral convection-enhanced delivery of topotecan with a subcutaneously implantable infusion pump. Neuro Oncol 2011;13:886–893.
120. Mehta AI, Choi BD, Ajay D, et al. Convection enhanced delivery of macromolecules for brain tumors. Curr Drug Discov Technol 2012;9:305–310.
121. Saito R, Bringas JR, McKnight TR, et al. Distribution of liposomes into brain and rat brain tumor models by convection-enhanced delivery monitored with magnetic resonance imaging. Cancer Res 2004;64:2572–2579.
122. Raghavan R, Mikaelian S, Brady M, Chen ZJ. Fluid infusions from catheters into elastic tissue: I. Azimuthally symmetric backflow in homogeneous media. Phys Med Biol 2010;55:281–304.
123. Mardor Y, Rahav O, Zauberman Y, et al. Convection-enhanced drug delivery: increased efficacy and magnetic resonance image monitoring. Cancer Res 2005;65:6858–6863.
124. Brady M, Raghavan R, Chen ZJ, Broaddus WC. Quantifying fluid infusions and tissue expansion in brain. IEEE Trans Biomed Eng 2011;58.
125. Sampson JH, Reardon DA, Friedman AH, et al. Sustained radiographic and clinical response in patient with bifrontal recurrent glioblastoma multiforme with intracerebral infusion of the recombinant targeted toxin TP-38: case study. Neuro Oncol 2005;7:90–96.
126. Mardor Y, Roth Y, Lidar Z, et al. Monitoring response to convection-enhanced taxol delivery in brain tumor patients using diffusion-weighted magnetic resonance imaging. Cancer Res 2001;61:4971–4973.
127. Sampson JH, Raghavan R, Provenzale JM, et al. Induction of hyperintense signal on T2-weighted MR images correlates with infusion distribution from intracerebral convection-enhanced delivery of a tumor-targeted cytotoxin. AJR Am J Roentgenol 2007;188:703–709.